PERGAMON

International Journal of Heat and Mass Transfer 41 (1998) 3829–3840

International Journal of HEAT and MASS TRANSFER

Enhancement of heat transfer in an inviscid-flow thermal boundary layer due to a Rankine vortex

Ricardo Romero-Méndez, Mihir Sen*, K. T. Yang, R. L. McClain

Department of Aerospace and Mechanical Engineering, University of Notre Dame, Notre Dame, IN 46556, U.S.A.

Received 7 August 1997; in final form 23 February 1998

Abstract

The effect on heat transfer of a Rankine vortex located near a flat plate is studied analytically. The velocity field is a superposition of an inviscid, uniform flow and a secondary perturbation created by the vortex. Three different vortex configurations are analyzed: transverse, longitudinal and normal with respect to the plate. In general, an increase in the local heat transfer coefficient is observed in the downwash and a decrease in the upwash regions. The transverse vortex leads to a larger increase than the longitudinal configuration. The normal vortex has a slight decrease in the heat transfer.

Nomenclature

a distance of vortex from leading edge [m]
b distance of vortex from plate [m]
L length of plate [m]
Nu local Nusselt number [m]
Pe Peclet number, $Pe = U\delta/\alpha$
Pe_L alternative Peclet number, $Pe_L = UL/\alpha$
r dimensionless radial coordinate
r_0 dimensionless radius of vortex core
R local heat transfer enhancement ratio
T dimensionless temperature
u, v, w dimensionless velocity components
U uniform velocity in x-direction [m s^{-1}]
x, y, z dimensionless Cartesian coordinates.

Greek symbols

α thermal diffusivity of fluid [m^2 s^{-1}]
Γ vortex circulation [m^2 s^{-1}]
δ scale of thermal boundary layer thickness, $\delta = \sqrt{\alpha L/U}$ [m]
ε small parameter, $\varepsilon = \Gamma/2\pi UL$
η dimensionless distance of vortex from plate, $\eta = b/L$
ξ dimensionless distance of vortex from leading edge, $\xi = a/L$.

Subscripts

v vortex-induced velocity
w wall
∞ ambient condition
0, 1, 2 order of perturbation term.

Superscripts

* dimensional quantities
$\overline{(\cdot)}$ average along constant z line
$\overline{\overline{(\cdot)}}$ average over square area around vortex.

1. Introduction

Hydrodynamic mixing in thermal boundary layers for the enhancement of convection heat transfer from solid boundaries is an artifice used in many compact heat exchangers. In a simplified sense, mixing may be thought of as due to the presence of small-scale vortical structures embedded within the thermal boundary layer. These vortices alter the heat transfer process by increasing the exchange of fluid between regions near and far from the wall. Often the vortices occur naturally due to turbulence; at other times they are caused by curvature of the streamlines such as the Taylor–Görtler vortices at concave surfaces, by thermal instabilities, or by flow around obstacles protruding from the wall. Sometimes they are introduced expressly for the purpose of enhancing heat transfer.

* Corresponding author. Tel.: 001 219 631 5975; fax: 001 219 631 8341; e-mail: msen@ovid.helios.nd.edu

0017–9310/98 $19.00
PII: S0017–9310(98)00094–S

Several researchers have studied the hydrodynamics of vortex generation as well as their thermal effect on heat transfer at a wall. Eibeck and Eaton [1] measured the effects of a longitudinal vortex embedded in a turbulent boundary layer. They found regions of increased and decreased heat transfer related to the downwash and upwash regions of the flow, respectively, but the net effect was to increase the heat transfer. Gentry and Jacobi [2] presented heat transfer results of the interaction of a delta-wing vortex generator and a laminar boundary layer in order to obtain a clearer understanding of the parameters involved in the design of vortex generators for heat exchanger applications. The use of other vortex generators for practical purpose has also been reported in the literature: Fiebig et al. [3] suggested the use of longitudinal vortex generators attached to fins in order to enhance heat transfer in plate-fin and tube heat exchangers, Zhu et al. [4] studied the longitudinal vortex generator interaction with turbulent channel flows, Tiggelbeck et al. [5] worked with channel flows with double rows of longitudinal vortex generators, Fiebig et al. [6] looked at compact plate heat exchangers with longitudinal vortex generators as fins, Fiebig et al. [7] analyzed a finned tube with longitudinal vortex generators, Kaniewski et al. [8] numerically computed mass transfer enhancement due to a longitudinal vortex, and Valencia et al. [9] studied the heat transfer enhancement by longitudinal vortices in a fin-tube heat exchanger.

Another type of vortex that occurs frequently in convective flows is the horseshoe vortex that is seen, for example, around the tubes of fin-tube heat exchangers. The vorticity in the hydrodynamic boundary layer that is formed on the fin is rolled up into a vortex which loops around the tube and trails off downstream. The horseshoe vortex enhances mixing in thermal boundary layers at the fin surface, thus improving the heat transfer characteristics of the heat exchanger. Baker [10] studied the hydrodynamics of the horseshoe vortex system in some detail. Saboya and Sparrow [11] measured mass transfer coefficients for a single-row plate and tube heat exchanger configuration using the naphthalene sublimation technique. Their measurements revealed the existence of a region of high mass transfer coefficient in a U-shaped band that coincides with the position of the horseshoe vortex. Ireland and Jones [12] used thermochromic liquid crystals to measure heat transfer around the base of a transverse cylinder between flat plates, confirming the dominant nature of the horseshoe vortex which enhances heat transfer to the wall in a localized region around the cylinder.

The purpose of the present work is to get an understanding of the vortex induced heat transfer enhancement process with emphasis on the effect of vortex geometry. This will help in the design and optimization of vortex generation devices in heat exchangers. The study of the influence of vortices on heat transfer has so far been either experimental or numerical rather than analytical, the principal obstacle being the complex nature of the hydrodynamics. However, even though it be approximate, analysis can lead to considerable insight on the physical mechanisms responsible for heat transfer enhancement. In the present work we will ignore the details of the vortex formation, but will assume its existence and then compute its effect on the heat transfer over a flat plate. We will solve the energy equation for a flow field produced by a uniform inviscid flow and a superposed Rankine vortex, an approximation which is strictly valid for a small Prandtl number. An analytical solution is made possible by a perturbation technique in which the nondimensional strength of the secondary vortex is the small parameter. The flow Peclet number will also be assumed to be large restricting us to a thin thermal boundary layer. The results will enable us to understand the interaction between the vortex motion and the thermal boundary layer over the plate, and the effect that this has on both local and overall changes in the heat transfer rate.

2. Velocity field

The physical problem to be analyzed is schematically shown in Figs 1(a), (b) and (c). A flat plate of finite dimension in the x-direction and infinite in the z-direction is submerged in a flow. We assume an inviscid, uniform flow of velocity U parallel to the plate. The incoming fluid is at a uniform temperature T^*_∞, and the flat plate is maintained at a constant temperature T^*_w so that a thermal boundary layer grows from the leading edge of the plate. A vortex is introduced in the flow over the plate in three different geometrical configurations: a transverse vortex shown in Fig. 1(a), a longitudinal vortex in Fig. 1(b), and a normal vortex in Fig. 1(c).

To avoid the singularity of the velocity field that would arise at the center of an inviscid vortex, we take it to be of the Rankine type which consists of a potential vortex surrounding a rigidly rotating core. The tangential velocity due to such a vortex is $\Gamma r^*/2\pi r^{*2}_0$ for $r^* < r^*_0$ and $\Gamma/2\pi r^*$ for $r^* \geqslant r^*_0$, where r^* is the radial distance from the vortex center and r^*_0 is the radius of the core. The strength of the vortex is Γ which is defined to be positive in the senses shown in Fig. 1. For the first two configurations, an image vortex of opposite sense located an equal distance below the plate is also needed for no-penetration through the plate.

2.1. Nondimensionalization

In the analysis that follows, two different characteristic lengths are used: the length of the plate L for the x- and z-coordinates, and a scale of the thermal boundary layer

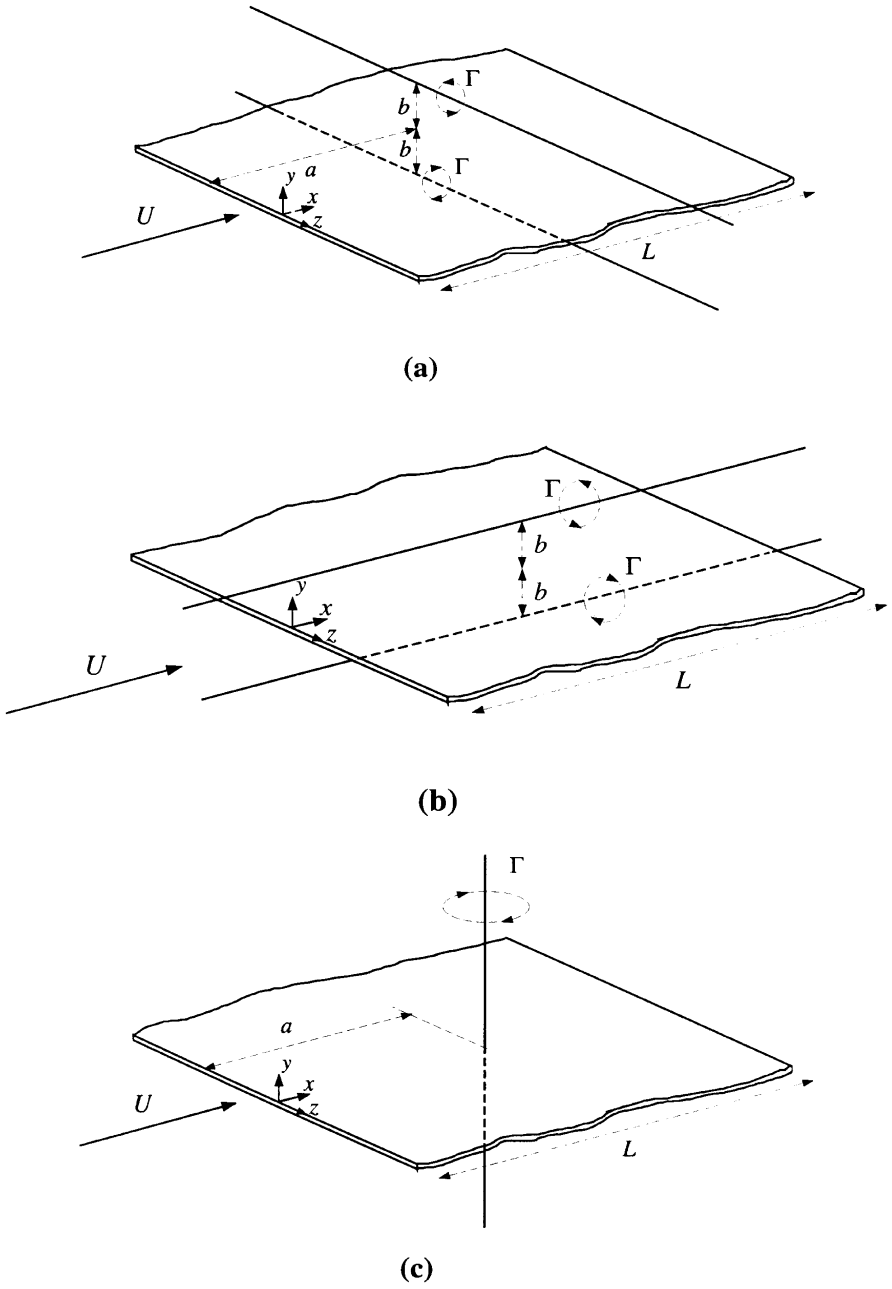

Fig. 1. Vortex geometries: (a) transverse; (b) longitudinal; and (c) normal.

thickness at the trailing edge of the plate, $\delta = \sqrt{\alpha L/U}$, for the y-coordinate, where α is the thermal diffusivity of the fluid. The proportional relationship between the x, y, z scales is $1 : Pe^{-1} : 1$, where the Peclet number is $Pe = U\delta/\alpha$. An alternative Peclet number could be defined as $Pe_L = UL/\alpha = Pe^2$. The velocity field is made dimensionless using U, U/Pe and U as scales for the u, v and w velocity components and the temperature of the fluid is nondimensionalized using $T(x, y, z) = (T^* - T^*_w)/(T^*_\infty - T^*_w)$.

The location of the vortices with respect to the plate is prescribed by two nondimensional coordinates. The different configurations are discussed below along with the flow field due to the vortex. The parameter

$\varepsilon = \Gamma/2\pi UL$ represents the strength of the vortex-induced secondary flow relative to the primary uniform velocity. The nondimensional core radius is $r_0 = r_0^*/L$.

2.2. Transverse vortex

The nondimensional coordinates $x = \xi$ and $y = Pe\,\eta$ fix the position of the center of the vortex, where $\xi = a/L$ and $\eta = b/L$. In nondimensional form the velocity field due to this vortex and its image is

$$u_v = -\frac{\varepsilon}{r_0^2}\frac{1}{Pe}(y - Pe\,\eta) + \varepsilon\,Pe\left[\frac{y + Pe\,\eta}{Pe^2(x-\xi)^2 + (y + Pe\,\eta)^2}\right] \tag{1}$$

$$v_v = \frac{\varepsilon}{r_0^2}(x-\xi) - \varepsilon\,Pe\left[\frac{Pe^2(x-\xi)}{Pe^2(x-\xi)^2 + (y + Pe\,\eta)^2}\right] \tag{2}$$

$$w_v = 0 \tag{3}$$

for $\sqrt{(x-\xi)^2 + (y/Pe - \eta)^2} < r_0$, and

$$u_v = \varepsilon\,Pe\left[-\frac{y - Pe\,\eta}{Pe^2(x-\xi)^2 + (y - Pe\,\eta)^2} + \frac{y + Pe\,\eta}{Pe^2(x-\xi)^2 + (y + Pe\,\eta)^2}\right] \tag{4}$$

$$v_v = \varepsilon\,Pe\left[\frac{Pe^2(x-\xi)}{Pe^2(x-\xi)^2 + (y - Pe\,\eta)^2} - \frac{Pe^2(x-\xi)}{Pe^2(x-\xi)^2 + (y + Pe\,\eta)^2}\right] \tag{5}$$

$$w_v = 0 \tag{6}$$

for $\sqrt{(x-\xi)^2 + (y/Pe - \eta)^2} \geqslant r_0$.

2.3. Longitudinal vortex

The center of this vortex is at $y = Pe\,\eta$ and $z = 0$. The resulting velocity field has the nondimensional velocity components

$$u_v = 0 \tag{7}$$

$$v_v = \frac{\varepsilon}{r_0^2}z - \varepsilon\frac{Pe^3\,z}{Pe^2\,z^2 + (y + Pe\,\eta)^2} \tag{8}$$

$$w_v = -\frac{\varepsilon}{r_0^2}\frac{1}{Pe}(y - Pe\,\eta) + \varepsilon\,Pe\frac{y + Pe\,\eta}{Pe^2\,z^2 + (y + Pe\,\eta)^2} \tag{9}$$

for $\sqrt{z^2 + (y/Pe - \eta)^2} < r_0$, and

$$u_v = 0 \tag{10}$$

$$v_v = \varepsilon\left[\frac{Pe^3\,z}{Pe^2\,z^2 + (y - Pe\,\eta)^2} - \frac{Pe^3\,z}{Pe^2\,z^2 + (y + Pe\,\eta)^2}\right] \tag{11}$$

$$w_v = \varepsilon\,Pe\left[-\frac{y - Pe\,\eta}{Pe^2\,z^2 + (y - Pe\,\eta)^2} + \frac{y + Pe\,\eta}{Pe^2\,z^2 + (y + Pe\,\eta)^2}\right] \tag{12}$$

for $\sqrt{z^2 + (y/Pe - \eta)^2} \geqslant r_0$.

2.4. Normal vortex

This vortex has its center at $x = \xi$ and $z = 0$. The velocity components of this vortex are

$$u_v = -\frac{\varepsilon}{r_0^2}z \tag{13}$$

$$v_v = 0 \tag{14}$$

$$w_v = \frac{\varepsilon}{r_0^2}(x-\xi) \tag{15}$$

for $\sqrt{(x-\xi)^2 + z^2} < r_0$, and

$$u_v = -\varepsilon\frac{z}{(x-\xi)^2 + z^2} \tag{16}$$

$$v_v = 0 \tag{17}$$

$$w_v = \varepsilon\frac{(x-\xi)}{(x-\xi)^2 + z^2} \tag{18}$$

for $\sqrt{(x-\xi)^2 + z^2} \geqslant r_0$. These velocity components are independent of Pe.

2.5. Large Pe approximation

For large Peclet numbers, the velocity field outside the core represented by equations (4)–(5) can be expanded as

$$u_v = \varepsilon\left[\frac{2\eta}{(x-\xi)^2 + \eta^2} - \frac{2\eta y^2[3(x-\xi)^2 + \eta^2]}{[(x-\xi)^2 + \eta^2]^3}Pe^{-2} + O(Pe^{-4}) + \cdots\right] \tag{19}$$

$$v_v = \varepsilon\left[\frac{4(x-\xi)y\eta}{[(x-\xi)^2 + \eta^2]^2} - \frac{8(x-\xi)y^3\eta[(x-\xi)^2 - \eta^2]}{[(x-\xi)^2 + \eta^2]^4}Pe^{-2} + O(Pe^{-4}) + \cdots\right] \tag{20}$$

for the transverse vortex. For the longitudinal vortex equations (11)–(12) become

$$v_v = \varepsilon\left[\frac{4zy\eta}{(z^2 + \eta^2)^2} - \frac{8zy^3\eta(z^2 - \eta^2)}{(z^2 + \eta^2)^4}Pe^{-2} + O(Pe^{-4}) + \cdots\right] \tag{21}$$

$$w_v = \varepsilon\left[\frac{2\eta}{z^2+\eta^2} - \frac{2\eta y^2(3z^2+\eta^2)}{(z^2+\eta^2)^3}Pe^{-2} + O(Pe^{-4}) + \cdots\right]. \quad (22)$$

The approximation is equivalent to assuming a thin thermal boundary layer, so that the physical location of the vortex core is outside this layer in the transverse and longitudinal cases.

3. Temperature field

The nondimensional equation governing the temperature distribution in an incompressible, constant-properties flow without viscous dissipation over a flat plate is

$$Pe^{-2}\frac{\partial^2 T}{\partial x^2} + \frac{\partial^2 T}{\partial y^2} + Pe^{-2}\frac{\partial^2 T}{\partial z^2} = u\frac{\partial T}{\partial x} + v\frac{\partial T}{\partial y} + w\frac{\partial T}{\partial z}. \quad (23)$$

This is an elliptic equation in all three Cartesian coordinates so that two boundary conditions must be supplied in each direction. In the longitudinal direction we have $T = 1$ at $x = 0$; we will not specify the condition at $x = 1$ because it will become irrelevant as soon as we drop the second derivative in x. In the normal direction the nondimensional fluid temperature is $T = 0$ at $y = 0$ and $T = 1$ for $y \to \infty$. In the transverse direction we will take $\partial T/\partial z = 0$ as $z \to \pm\infty$. These conditions enable the temperature field for a two-dimensional flat plate thermal boundary layer to be recovered in the absence of the vortex.

For a thermal boundary layer to exist in the unperturbed flow, the Peclet number must be large. Under this condition the second derivatives in x and z can be dropped from the equation, and it becomes parabolic in both these directions. Not all temperature boundary conditions can now be satisfied. In the main flow direction, the only condition that will be satisfied is $T = 1$ at $x = 0$ as long as the flow velocity is everywhere positive, a condition which holds if $\varepsilon \leqslant r_0$. In fact, the plate could be of infinite length in the x-direction without changing the temperature field that we will calculate here. The matter is slightly different in the z-direction. For the transverse vortex, there is no temperature variation in z so that $\partial T/\partial z = 0$ everywhere. For the other two configurations, the perturbation velocity field will asymptote to zero as $z \to \pm\infty$, so that the two-dimensional thermal boundary layer is again recovered. Even though the equation is first-order in z, both boundary conditions in that direction can be satisfied. In addition to these boundary conditions, we assume that in the transverse and longitudinal configurations the core of the vortex and that of its image do not touch, implying that $r_0 < \eta$.

As a result of these approximations, we have

$$\frac{\partial^2 T}{\partial y^2} = u\frac{\partial T}{\partial x} + v\frac{\partial T}{\partial y} + w\frac{\partial T}{\partial z}. \quad (24)$$

The velocities derived from a superposition of the uniform and vortex flows can be expressed as $u = 1+\varepsilon u'$, $v = \varepsilon v'$, $w = \varepsilon w'$, where $(u', v', w') = (u_v, v_v, w_v)/\varepsilon$. Note that the velocity field is two-dimensional for the transverse and normal vortices, and three-dimensional for the longitudinal one. The temperature field is also two-dimensional for the transverse vortex, but is three-dimensional for the other two geometries.

The linear equation (24) with its corresponding boundary conditions can be solved by the method of perturbations if we assume that ε is small, u', v' and w' are of order unity, and $Pe^{-1} \ll \varepsilon$. The last assumption makes the Peclet number contribution negligibly small in equations (19)–(22). We propose a solution of the form

$$T(x, y, z) = T_0(x, y, z) + \varepsilon T_1(x, y, z) + \varepsilon^2 T_2(x, y, z) + \cdots \quad (25)$$

where we will include only three terms of the series; this will be sufficient to include all the qualitative physics in the problem. T_i $(i = 0, 1, 2)$ are independent of the flow parameters ε and Pe.

3.1. $O(\varepsilon^0)$ solution

Collecting terms of order ε^0 we have

$$\frac{\partial^2 T_0}{\partial y^2} - \frac{\partial T_0}{\partial x} = 0 \quad (26)$$

subject to $T_0(0, y, z) = 1$, $T_0(x, 0, z) = 0$ and $T_0(x, \infty, z) = 1$. The solution is

$$T_0(x, y, z) = \frac{2}{\sqrt{\pi}}\int_0^{y/2\sqrt{x}} e^{-\tau^2}\,d\tau. \quad (27)$$

To this order the temperature field represents a growing thermal boundary layer at the plate, unperturbed by the presence of the vortex.

3.2. $O(\varepsilon)$ solution

We have

$$\frac{\partial^2 T_1}{\partial y^2} - \frac{\partial T_1}{\partial x} = -f_1(x, y, z) \quad (28)$$

where

$$f_1(x, y, z) = -\left(u'\frac{\partial T_0}{\partial x} + v'\frac{\partial T_0}{\partial y}\right) \quad (29)$$

subject to $T_1(x, 0, z) = 0$, $T_1(x, \infty z) = 0$ and $T_1(0, y, z) = 0$. The inhomogeneous term $f_1(x, y, z)$ is a heat source for the thermal boundary layer at this order.

It represents the effect of the vortical velocities on the unperturbed temperature field.

Equation (28) can be solved using a Green's function. The solution is

$$T_1(x,y,z) = \frac{1}{2\sqrt{\pi}}\int_0^x\int_0^\infty (x-x')^{-1/2}\left[\exp\left(-\frac{(y-y')^2}{4(x-x')}\right) - \exp\left(-\frac{(y+y')^2}{4(x-x')}\right)\right] f_1(x',y',z)\,\mathrm{d}x'\,\mathrm{d}y'. \quad (30)$$

3.3. $O(\varepsilon^2)$ solution

To this order

$$\frac{\partial^2 T_2}{\partial y^2} - \frac{\partial T_2}{\partial x} = -f_2(x,y,z) \quad (31)$$

where

$$f_2(x,y,z) = -\left(u'\frac{\partial T_1}{\partial x} + v'\frac{\partial T_1}{\partial y} + w'\frac{\partial T_1}{\partial z}\right) \quad (32)$$

subject to $T_2(x,0,z) = 0$, $T_2(x,\infty,z) = 0$ and $T_2(0,y,z) = 0$. The source $f_2(x,y,z)$ now includes the effect of advection of the once-perturbed temperature field $T_1(x,y,z)$. The solution of equation (31) is similar to equation (30) but with subscript 2 instead of 1.

4. Heat transfer rates

The local Nusselt number representing the dimensionless heat transfer rate from the plate can be expressed as

$$Nu(x,z) = Nu_0(x,z) + \varepsilon Nu_1(x,z) + \varepsilon^2 Nu_2(x,z) + \cdots \quad (33)$$

where

$$Nu_i(x,z) = \left.\frac{\partial T_i}{\partial y}\right|_{y=0} \quad \text{for } i = 0,1,2,\ldots.$$

The local Nusselt numbers can be determined from the computed temperature fields as

$$Nu_0(x,z) = \frac{1}{\sqrt{\pi x}} \quad (34)$$

$$Nu_i(x,z) = \frac{1}{2\sqrt{\pi}}\int_{x'=0}^x\int_{y'=0}^\infty \frac{y'}{(x-x')^{3/2}} \times \exp\left(-\frac{y'^2}{4(x-x')}\right) f_i(x',y',z)\,\mathrm{d}x'\,\mathrm{d}y' \quad (35)$$

where $i = 1,2,\ldots.$

To obtain an average Nusselt number along a strip, we integrate $Nu_i(x,z)$ in one coordinate direction. Averaging only in the x-direction, we get

$$\overline{Nu}_i(z) = \int_0^1 Nu_i(x,z)\,\mathrm{d}x \quad (36)$$

$\overline{Nu}_i(z)$ then represents the z-variation of the Nusselt number. Since the plate is infinite in the z-direction, the effect of a longitudinal or normal vortex averaged over the entire area would be zero. For the purpose of quantifying the effect of the vortex, we have chosen a square area $0 \leqslant x \leqslant 1$, $-0.5 \leqslant z \leqslant 0.5$ directly around the vortex location to perform the averaging. This area-averaged Nusselt number is then given by

$$\overline{\overline{Nu}}_i = \int_{-0.5}^{0.5}\int_0^1 Nu_i(x,z)\,\mathrm{d}x\,\mathrm{d}z. \quad (37)$$

From equation (34) we get

$$\overline{\overline{Nu}}_0 = \frac{2}{\sqrt{\pi}} \quad (38)$$

for the unperturbed thermal boundary layer.

We also define $R(x,z)$ as the local heat transfer enhancement ratio, i.e. the relative increase of the local heat transfer rate caused by the addition of the secondary vortex flow. Thus,

$$R(x,z) = \frac{Nu(x,z) - Nu_0(x)}{Nu_0(x)}. \quad (39)$$

Again, one overbar indicates an integral with respect to z, and two over the square area below the vortex.

5. Results

The perturbation terms can be evaluated to any order, the only time-consuming computation being in the evaluation of the multiple integrals which appear, which was done using the trapezoidal rule. The perturbation results are validated by comparison with a numerical solution of equation (24), based on a second-order, implicit, finite-difference method, applied to the two-dimensional transverse vortex configuration. Table 1 shows a comparison between R obtained from the perturbation and numerical procedures. The values are in good agreement and become closer as the number of terms of the perturbation is increased.

The perturbation results for each one of the three vortex geometries are discussed below. In each case Γ, and hence ε, is understood to be positive; for negative ε the physical sense of rotation of the vortex would be opposite to the ones shown in Fig. 1. From the physics of the flow it is obvious that the direction of rotation makes a difference to the area-averaged heat transfer rates only for the transverse vortex, but not for the longitudinal and normal vortices. This is confirmed in the perturbation solutions by the presence and absence, respectively, of terms corresponding to the odd powers of ε.

Table 2 shows the small effect that a change in r_0 has

Table 1
Comparison of two- and three-term results of $R(x)$ for a transverse vortex with a numerical solution of equation (24); $Pe = 1000$, $\varepsilon = 0.05$, $r_0 = 0.1$, $\eta = 0.2$, $\tau = 0.5$

	$R(x) \times 10$		
x	Two terms	Three terms	Numerical
0.1	0.58424	0.56851	0.57293
0.2	1.01964	0.98052	0.98899
0.3	1.82511	1.72540	1.73916
0.4	3.09188	2.85308	2.88235
0.5	3.81044	3.42856	3.48398
0.6	2.62252	2.35651	2.39727
0.7	1.08968	1.03547	1.03328
0.8	0.18131	0.24873	0.22469
0.9	−0.27521	−0.15882	−0.17455
1.0	−0.49943	−0.36913	−0.35344

Table 2
Effect of r_0 on $\overline{\overline{R}}$; $Pe = 1000$, $\varepsilon = 0.05$, $\eta = 0.2$, $\xi = 0.5$

	$\overline{\overline{R}}$	
Configuration	$r_0 = 0.1$	$r_0 = 0.05$
Transverse	1.165×10^{-1}	1.165×10^{-1}
Longitudinal	4.311×10^{-2}	4.313×10^{-2}
Normal	-2.242×10^{-3}	-2.534×10^{-3}

on $\overline{\overline{R}}$ for the three vortex configurations. For the transverse and longitudinal vortices, the heat transfer rate is not seriously affected by r_0 as the vortex core is mostly outside of the thermal boundary layer. For the normal vortex the influence is slightly larger with a decrease of $\overline{\overline{R}}$ as r_0 is increased. For simplicity, we will take $r_0 = 0.1$ for the rest of the study.

5.1. Transverse vortex

For the transverse vortex, the velocity and temperature fields are two-dimensional and do not vary with z; the local Nusselt number is thus only a function of x. $Nu_0(x)$ is the thermal boundary layer solution for uniform flow; $Nu_1(x)$ is the lowest order term that contains the effect of the vortex. The contribution of the $\varepsilon^2 Nu_2(x)$ term to the heat transfer is smaller as shown in Table 1.

Figure 2 shows the change of the temperature field due to a vortex at $x = \xi = 0.5$ calculated using two terms of the perturbations series. In the downwash side of the vortex, e.g. at $x = 0.3$, the profile of the temperature relative to the unperturbed value has a positive slope near the wall which contributes to an increase in heat transfer. The slope of the temperature change grows to a maximum at the point where the vortex is located, i.e. $x = \xi$. In the upwash side of the vortex, the slope at the wall decreases and becomes zero around $x = x_c$, which for these parameters is 0.83, at which point the local heat transfer does not change due to the presence of the vortex. Further downstream, for instance at $x = 0.95$, the slope of $T - T_0$ at the wall becomes negative and the heat transfer decreases because of the thickening effect of the upwash.

Figure 3 shows the x dependence of the local heat transfer enhancement ratio, R. The secondary flow contributes to an increase in the heat transfer in the downwash side, $x < \xi$, of the vortex. On the upwash side there is an increase in the region $x_c > x > \xi$, and a decrease in $x_c < x$. The curves are not anti-symmetric with respect to the position of the vortex core at $x = \xi$ due to the main flow which advects hot fluid from the upstream to the downstream side of the vortex. Thus, the area-averaged heat transfer enhancement, $\bar{R}$, is positive even though there are regions where the heat transfer is locally reduced. Vortex rotation in the opposite direction to that shown in Fig. 1(a) leads to an overall decrease in heat transfer.

Figure 4 shows $\bar{R}$ as a function of the position η for all other parameters fixed. An η increases, the vortex moves away from the wall and its effect decreases.

5.2. Longitudinal vortex

The flow and temperature fields are three-dimensional so that $Nu = Nu\ (x, z)$. Figure 5(a) shows the contribution to heat transfer enhancement from the $O(\varepsilon)$ term. Again the regions of increased or decreased heat transfer correspond to regions of downwash or upwash secondary flow. There is anti-symmetry about the vortex position so that the area-averaged heat transfer increase to this order is zero, and one must go to higher orders to perceive any change. Figure 5(b) shows the $O(\varepsilon^2)$ term where the effect of advection of the once-perturbed temperature field gives regions of positive or negative contribution. The $O(\varepsilon^2)$ term is negative for large positive or negative z where colder fluid is brought to hotter regions, and positive near the middle of the plate just below the vortex location where hot fluid is advected into colder regions thus reducing the thickness of the thermal boundary layer. The shape of the $O(\varepsilon^2)$ contribution surface has symmetry with respect to $z = 0$ and results in a non-zero area average. The overall effect of this vortex is an increase of the area-averaged heat transfer. Eibeck and Eaton [1] report experimental results that are qualitatively similar.

Figure 6 shows $\overline{\overline{R}}$ vs. η. As in Fig. 4 for the transverse vortex, $\overline{\overline{R}}$ decreases monotonically as η becomes larger for exactly the same reason.

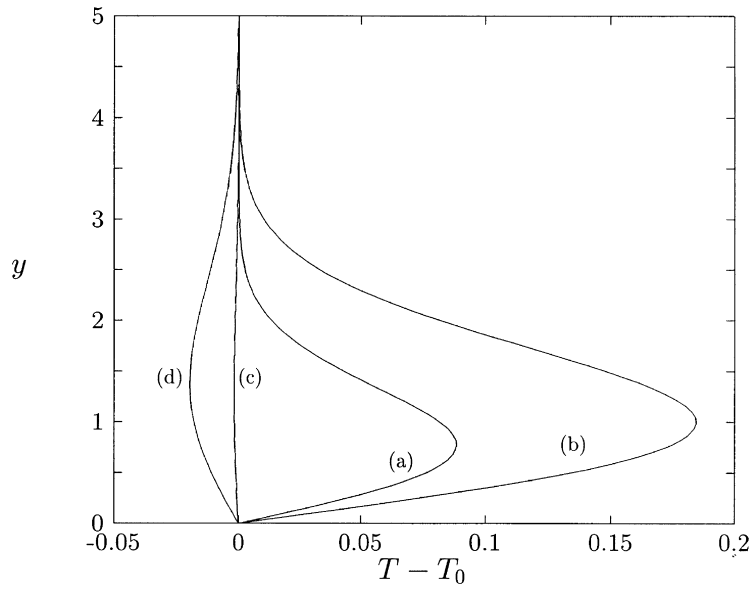

Fig. 2. $T-T_0$ vs. y for transverse vortex: $Pe = 1000$, $\varepsilon = 0.05$, $r_0 = 0.1$, $\eta = 0.2$, $\xi = 0.5$; (a) $x = 0.3$, (b) $x = 0.5$, (c) $x = 0{,}83$, and (d) $x = 0.95$.

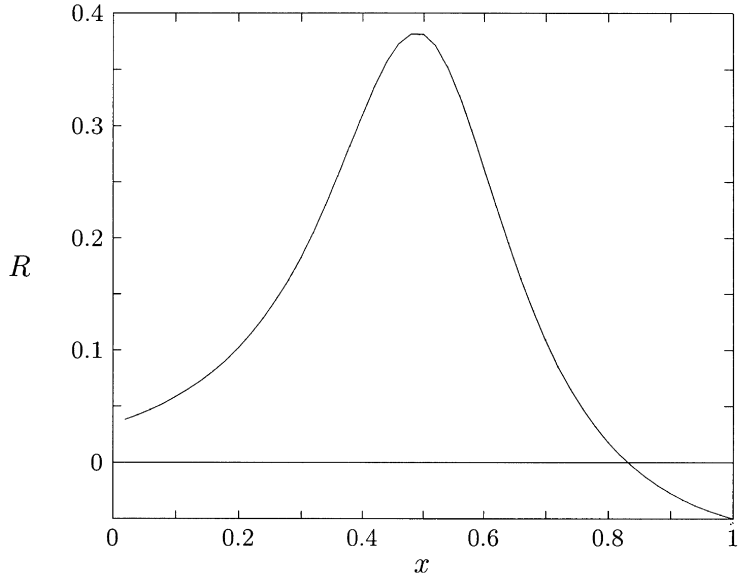

Fig. 3. R vs. x for transverse vortex; $Pe = 1000$, $\varepsilon = 0.05$, $r_0 = 0.1$, $\eta = 0.2$, $\xi = 0.5$.

5.3. Normal vortex

In this vortex, the absence of a secondary velocity component normal to the wall reduces the effect that the vortex has on heat transfer. Compared to the previous two geometries, the local heat transfer change is very small.

Figure 7(a) shows the spatial variation of the contribution of the $O(\varepsilon)$ term to the heat transfer. We observe regions of decreased heat transfer for $z > 0$ and increased

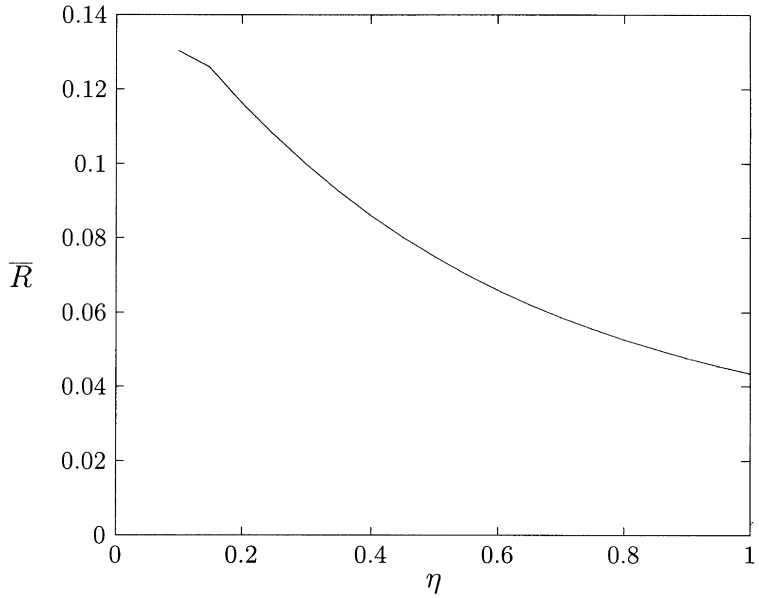

Fig. 4. $\bar{R}$ vs. η for transverse vortex; $Pe = 1000$, $\varepsilon = 0.05$, $r_0 = 0.1$, $\xi = 0.5$.

heat transfer for $z < 0$. Reduction in heat transfer is not due to upwash flows which do not exist here, but is rather caused by the secondary advection in a direction opposite to the main flow direction. Conversely, the region of increased heat transfer is where a secondary flow advects fluid in the same direction as the main flow. Both effects are more important in the neighborhood of the vortex and just downstream of it. Due to anti-symmetry, however, the contribution of the $O(\varepsilon)$ term to $\overline{\overline{R}}$ is zero. Figure 7(b) shows the contribution of the $O(\varepsilon^2)$ term. The region upstream of the vortex has decreased heat transfer due to transverse advection of fluid from regions where the boundary layer has been thickened by the $O(\varepsilon)$ term. The region downstream of the vortex is mainly that of increased heat transfer due to transverse advection from regions where the boundary layer is thinner as a result of the $O(\varepsilon)$ temperature field. The sides of the plate are also regions of negative $O(\varepsilon^2)$ contribution as fluid is advected from regions that are colder as a result of the $O(\varepsilon)$ solution. The $O(\varepsilon^2)$ term is symmetric about $z = 0$ leading to a nonzero value of $\overline{\overline{R}}$. The area-averaged effect is negative because the heat transfer is increased only in a narrow region downstream of the vortex.

Figure 8 illustrates how $\overline{\overline{R}}$ depends on ξ. It is observed that higher heat transfer reduction occurs for a normal vortex near the leading edge. The thickening of the thermal boundary layer downstream leads to a smaller temperature gradient and a decrease in the heat transfer reduction due to advection.

6. Conclusions

The effect on heat transfer due to the presence of a Rankine combined vortex near a plane wall has been analytically determined by a perturbation analysis. For purposes of the analysis we have assumed a small vortex strength and large Peclet number; i.e. specifically we have taken $\varepsilon \ll 1$, $Pe \gg 1$ and $\varepsilon\ Pe \gg 1$. For transverse and longitudinal vortices, the fluid in some regions of the flow moves towards the wall increasing the local heat transfer, and in other regions moves away decreasing it. The heat transfer is thus locally inhibited in some places and enhanced at others. However, the increase and decease are not necessarily symmetric with respect to vortex position. The component of the flow that displaces fluid between upwash and downwash regions is partly responsible for the asymmetries, which are then responsible for an increase in the area-averaged heat transfer rates. The normal vortex is different; the advection occurs in planes parallel to the plate and there is a reduction of the area-averaged heat transfer due to a modification of the flow velocity.

The role of the secondary flow differs for each vortex configuration. For the transverse vortex, the main flow is responsible for the displacement of fluid between the downwash and upwash regions, while in the longitudinal vortex this role is played by the secondary flow, so that its influence is small. Hence the strongest influence on the area-averaged heat transfer is in the transverse vortex

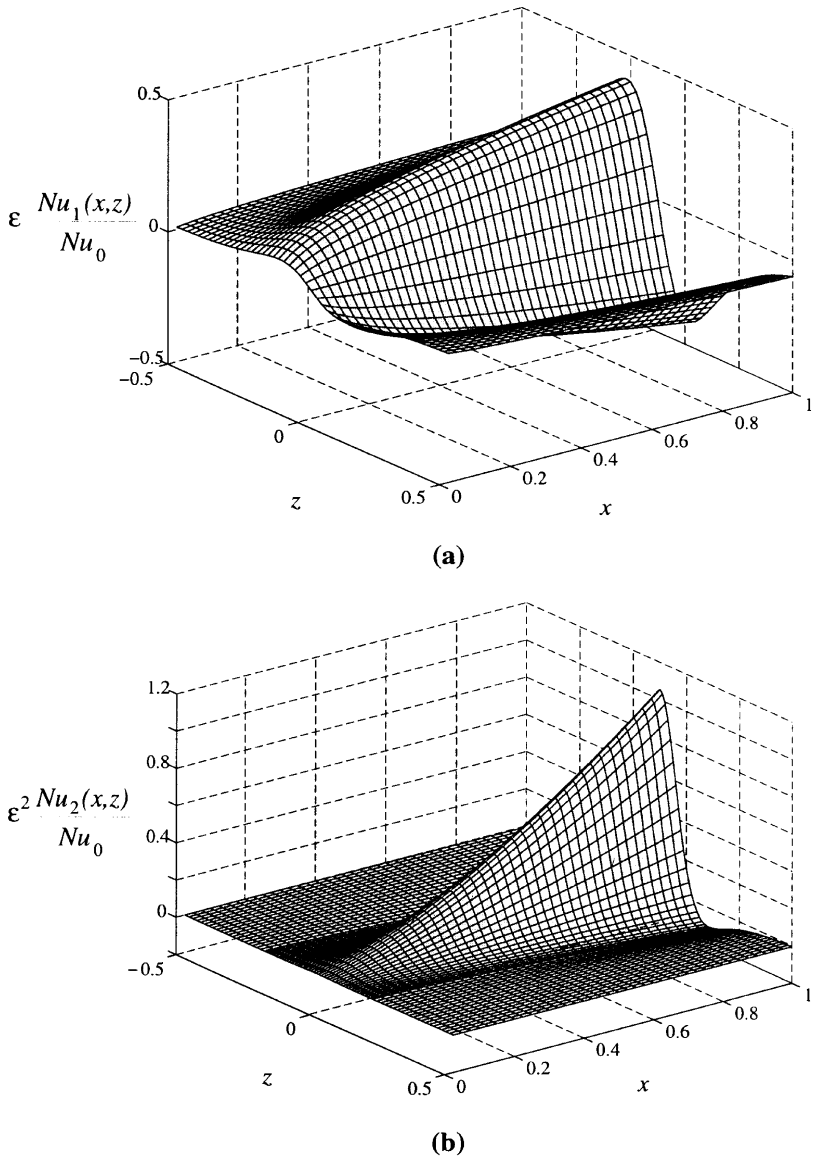

Fig. 5. Contribution to heat transfer enhancement for longitudinal vortex: $Pe = 1000$, $\varepsilon = 0.05$, $r_0 = 0.1$, $\eta = 0.2$; (a) $O(\varepsilon)$, (b) $O(\varepsilon^2)$.

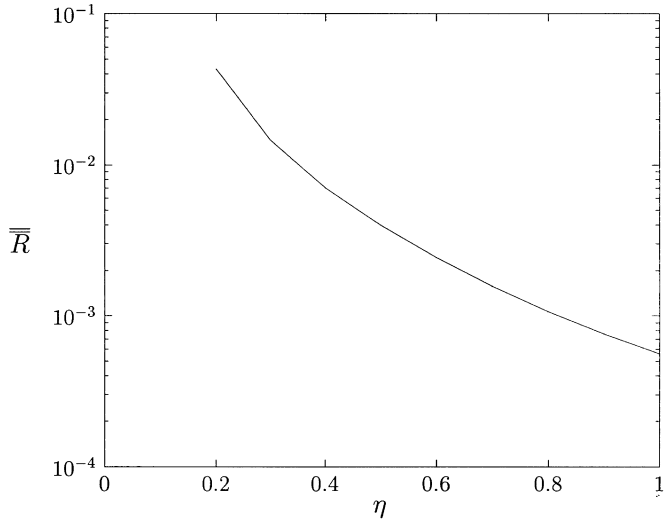

Fig. 6. $\overline{\overline{R}}$ vs. η for longitudinal vortex; $Pe = 1000$, $\varepsilon = 0.05$, $r_0 = 0.1$.

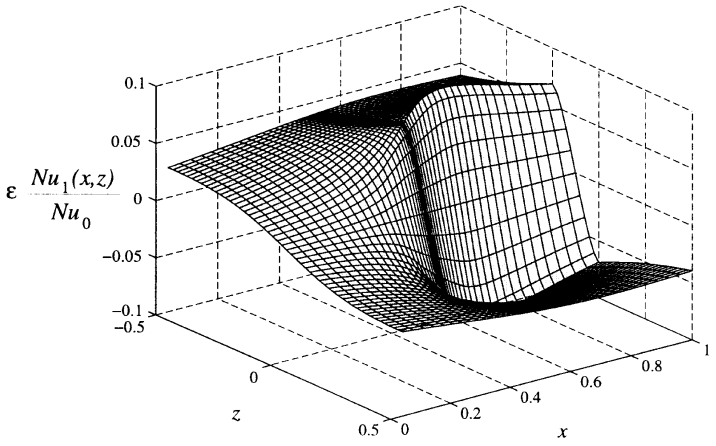

(a)

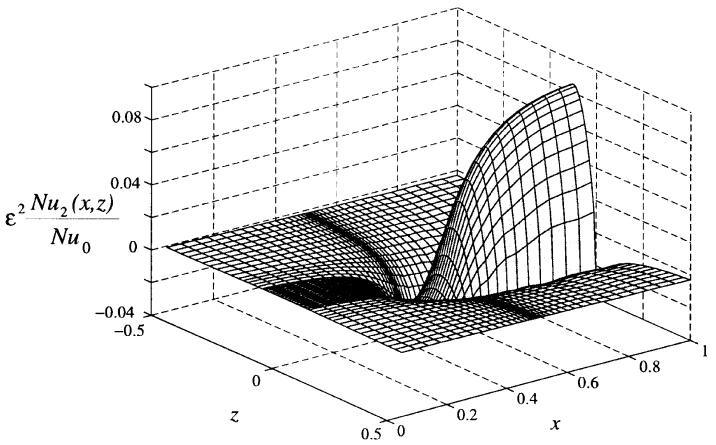

(b)

Fig. 7. Contribution to heat transfer enhancement for normal vortex: $Pe = 1000$, $\varepsilon = 0.05$, $r_0 = 0.1$, and $\xi = 0.5$; (a) $O(\varepsilon)$, (b) $O(\varepsilon^2)$.

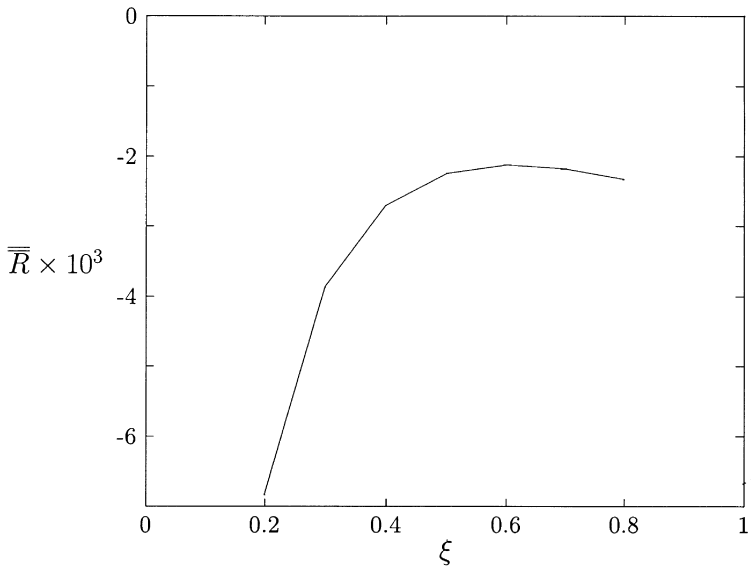

Fig. 8. $\overline{\overline{R}}$ vs. ξ for normal vortex; $Pe = 1000$, $\varepsilon = 0.05$, $r_0 = 0.1$.

where most of the area-averaged heat transfer enhancement comes from the $O(\varepsilon)$ term. The longitudinal vortex has a weaker effect since the $O(\varepsilon)$ contribution vanishes due to anti-symmetry and the first non-zero contribution comes from the $O(\varepsilon^2)$ term. For the normal vortex, the change is considerably smaller than for the other configurations since the velocity component normal to the plate is absent.

Acknowledgments

The authors would like to thank Mr D. K. Dorini and BRDG-TNDR Corporation for their interest in this research, and in the establishment of the Hydronics Laboratory at the University of Notre Dame. R.R.-M. acknowledges the sponsorship of the Government of Mexico through a CONACYT-Fulbright Fellowship. We are also grateful for the helpful comments of an anonymous reviewer.

References

[1] Eibeck PA, Eaton JK. Heat transfer effects of a longitudinal vortex embedded in a turbulent boundary layer. ASME Journal of Heat Transfer 1987;109:16–24.
[2] Gentry MC, Jacobi AM. Heat transfer enhancement by delta-wing vortex generators on a flat plate: vortex interactions with the boundary layer. Experimental Thermal and Fluids Science 1997;14:231–42.
[3] Fiebig M, Brockmeier U, Mitra NK, Guentermann T. Structure of velocity and temperature fields in laminar channel flows with longitudinal vortex generators. Numerical Heat Transfer 1989;15(3):281–302.
[4] Zhu JX, Mitra NK, Fiebig M. Effects of longitudinal vortex generators on heat transfer and flow loss in turbulent channel flows. International Journal of Heat and Mass Transfer 1993;36:2339–47.
[5] Tiggelbeck S, Mitra NK, Fiebig M. Experimental investigations of heat transfer enhancement and flow losses in a channel with double rows of longitudinal vortex generators. International Journal of Heat and Mass Transfer 1993;36:2327–37.
[6] Fiebig M, Guentermann T, Mitra NK. Numerical analysis of heat transfer and flow loss in a parallel plate heat exchanger element with longitudinal vortex generators as fins. ASME Journal of Heat Transfer 1995;117:1064–7.
[7] Fiebig M, Chen Y, Grosse-Gorgemann A, Mitra NK. Conjugate heat transfer of a finned tube part B: heat transfer augmentation and avoidance of heat transfer reversal by longitudinal vortex generators. Numerical Heat Transfer, Part A—Applications 1995;28:147–55.
[8] Kaniewski M, Hanne HW, Mitra NK. Mass transfer enhancement by longitudinal vortices. Heat and Mass Transfer 1997;32:163–6.
[9] Valencia A, Fiebig M, Mitra NK. Heat Transfer enhancement by longitudinal vortices in a fin-tube heat exchanger with flat tubes. ASME Journal of Heat Transfer 1996;118:209–11.
[10] Baker CJ. The laminar horseshoe vortex. Journal of Fluid Mechanics 1979;95:347–67.
[11] Saboya FEM, Sparrow EM. Local and average transfer coefficients for one-row plate fin and tube heat exchanger. ASME Journal of Heat Transfer 1974;96:265–72.
[12] Ireland PT, Jones TV. Detailed measurements of heat transfer on and around a pedestal in fully developed passage flow. Proceedings of the Eighth International Heat Transfer Conference, Vol. 3. Washington, DC: Hemisphere, 1986;975–80